South African Journal of Geomatics, Vol. 10. No. 2, August 2021

Hydrological Impacts of Land Use - Land Cover Change on Urban Flood Hazard: A Case Study of the Jukskei River in Alexandra Township, Johannesburg, South Africa.

Tshepo Sylvester Mawasha[1] and Wilma Britz[2]

Department of Geoscience, Nelson Mandela University, Port Elizabeth, South Africa
[1] tshepo_mawasha@yahoo.com, [2] wilma.britz@mandela.ac.za

DOI: http://dx.doi.org/10.4314/sajg.v10i2.11

Abstract

Flooding in urban areas is a major natural disaster causing damage to infrastructure, properties and loss of life. In urban areas the major causes behind the changing hydrological processes (i.e., floods) include topography, increase in precipitation due to climate change and change in land-use/land-cover (LULC) over time. The objective of this study is to evaluate the spatial and temporal LULC change impacts on flooding along the Jukskei River in Alexandra Township, Johannesburg, South Africa. The LULC images of 1987 MSS and 2015 OLI derived from Landsat satellite were pre-processed and classified using a supervised classification method. The analysis of LULC revealed that, there is an increase in built-up area from 934,2 ha to 1277,2 ha and reduction in intact and sparse vegetation from 190,5 ha to 62,4 ha and 380,8 ha to 142,1 ha, respectively, between the years 1987 and 2015. The flood depth map, velocity map and flood depth-velocity for different return periods and LULC scenarios have been developed by using an integrated approach of the Hydrological Engineering Centre-River Analysis System (HEC-RAS) and the HEC-GeoRAS with the geographic information system (GIS) and remote sensing data. From the analysis, it is observed that there is an increase in flood depth and flood velocity from 2,3 m to 3,0 m and 1,4 m/s to 3,4 m/s, whereas the depth-velocity for the last 28-years increased by 3,4 m^2/s from 2,9 m^2/s to 6,3 m^2/s for the 1987 LULC and the 2015 LULC conditions, respectively. The flood hazard maps generated in this study can be used by local authorities and municipalities for flood disaster management.

Keywords: *LULC change, GIS and remote-sensing, HEC-RAS/HEC-GeoRAS, Hydrological modelling, flood hazard mapping*

1. Introduction

In recent years, there has been a significant increase in the frequency of flood occurrence in developed and developing countries. The frequency of floods and the number of flood damages shows an increasing trend through the 20th century (Parry *et al.,* 2007; Lugeri *et al.,* 2010). Historically, the Jukskei River in Alexandra Township located northwest of Johannesburg in South Africa, has witnessed a series of floods that have resulted in widespread destruction. Alexandra Township is one of the densely populated townships in Johannesburg and prone to flooding during the rainfall season.

However, the majority of the people within Alexandra township are residing on any available land space along the Jukskei River, which alters the land-use/land-cover (LULC) characteristics of the area. The impact of LULC change on the hydrological process is the main reason for urban flooding (Stonestrom *et al.,* 2009; Wagner *et al.,* 2013). The LULC change increases the total runoff volume and peak discharge of storm runoff events (Dewan and Yamaguchi, 2009; Ali *et al.,* 2011; Sayal *et al.,* 2014). Moreover, the LULC change is influenced by humans trying to meet various needs such as residential, industrial, agricultural, mining and other infrastructural facilities and there are major concerns associated with the economic and sustainable growth of an area (Zubair, 2006; Rawat *et al.,* 2013).

Youssef *et al.* (2009) mentioned that due to heavy rains, there are land-use change in basin areas and other engineering applications that all add to the frequency and greatness of flood events. There is a high increase in the need for effective modelling to understand the problem to mitigate flash floods' disastrous effects. The integration of GIS techniques with the Hydrological Engineering Centre – River Analysis System (HEC-RAS) and the Hydrological Engineering Centre – Geographical River Analysis System (HEC-GeoRAS) in modelling floodplain areas has become one of the popular methods used among researchers nowadays (Sulaiman *et al.,* 2014). In recent years, the use of GIS has grown rapidly in hydrology management and research. The main advantage of using GIS for flood management is that it not only generates a visualization of flooding, but also creates potential to further analyse and estimate probable damage due to a flood (Hausmann and Weber, 1988; Clark, 1998). Werner (2001) stated that, the end result of the process is not only quicker floodplain delineation with greater accuracy than traditional methods, but a flow depth grid could also be extracted, indicating the level of inundation in the floodplain.

Al-Rawas *et al.* (2015) took advantage of GIS data about land-use changes to examine peak-flow and time-to-peak by mimicking local flash floods. Fosu *et al.* (2013) have suggested an approach for river inundation and hazard mapping with the help of GIS, spatial technology and HEC-RAS hydraulic tools. Affected buildings were delineated by overlaying the flooded area onto the topographic maps. They concluded that high water depth occurs along the main channel and spreads gradually to the flood plain. Salimi *et al.* (2008) integrated the hydraulic simulation model HEC-RAS with GIS for a delineation of flood depth and the extent for the catchment of the Zaremroud River in Iran. The results revealed that for flood plain management, the integration of hydraulic simulation with GIS is very effective. Ahmad *et al.* (2010) generated a flood hazard map for Nullah Lai in Rawalpindi, Pakistan using HEC-RAS and HEC-GeoRAS hydrological models with GIS. They found a relationship between inundation depth and specific discharge value.

In this research, the main objective is to assess the effect of LULC change to hydrological response within the floodplain area based on the integration of HEC-RAS/HEC-GeoRAS with GIS and remote sensing techniques. The flood depth extents, flow velocity and depth-velocity maps for the LULC patterns of 1987 and 2015 were developed for 2, 25 and 100-year return periods. The results of this research can be used by disaster management authorities and societies for early evacuation planning,

flood impact mitigation, and identifying properties and infrastructure that might be at risk of being affected by a flood.

2. Study area

Alexandra Township (Figure 1) bound between latitudes 26°05'00.9"S and 26°06'59.9"S and longitudes 28°05'08.8"E and 28°06'15.2"E about ± 11 km northwest of Johannesburg in South Africa. Alexandra Township falls within the Jukskei River catchment area, which is one of the largest catchments in Gauteng province. The southern area is densely populated, urbanized and heavily industrialised, whereas the northern part consists mainly of open space area. The area has a relatively dry and sunny climate with a maximum precipitation that occurs in summer and a minimum precipitation in spring. The mean annual rainfall within the catchment area is relatively uniform. However, most of the rainfall (70% to 90%) is received during the raining season and usually covers the months from September to March with a mean annual rainfall that ranges from 650 mm to 900 mm (City of Johannesburg, 2008). The average minimum and maximum temperatures during summer season range between 16º C and 25º C, respectively; while during the winter season the temperature averages about 13º C to below freezing point (Mucina and Rutherford, 2006). The Jukskei River which passes through Alexandra Township covers a length of 390 km, originates from Betrams, next to Johannesburg CBD flowing to the North and draining into the Crocodile River. For the purpose of this study, the length of the river reach selected covers 3,8 km of the Jukskei River within Alexandra Township. The selected river reach within the Alexandra Township is where floods frequently occur, which cause a great damage, loss of property and risk of people's lives.

3. Description of the hydraulic and hydrological model

The Hydrological Engineering Centre River Analysis System (HEC-RAS) is a hydrodynamic model that has capabilities to perform one-dimensional hydraulic calculations of water surface profiles in various channel networks using St. Venant equations when flow conditions are approximated as unidirectional (Lastra *et al.,* 2008). The HEC-RAS is a widely used software application that can perform one and two-dimensional hydraulic calculations for a full network of natural and constructed channels, overbank/floodplain areas and levee protected areas (HEC, 2005). It is viewed as the most widely used floodplain hydraulic model in the world with constant upgrades (Dyhouse *et al.,* 2003). In this research study, the Jukskei River area in Alexandra Township is assumed to have a steady flow river. A steady flow river can be defined as the river which has assumed to flow steadily along the reach as the energy equation does not include time dependent flows (Salimi *et al.,* 2008). According to Salimi *et al.* (2008) the solution of a one-dimensional energy equation is used as the basic computational procedure in the HEC-RAS model. The energy equation is written as follows:

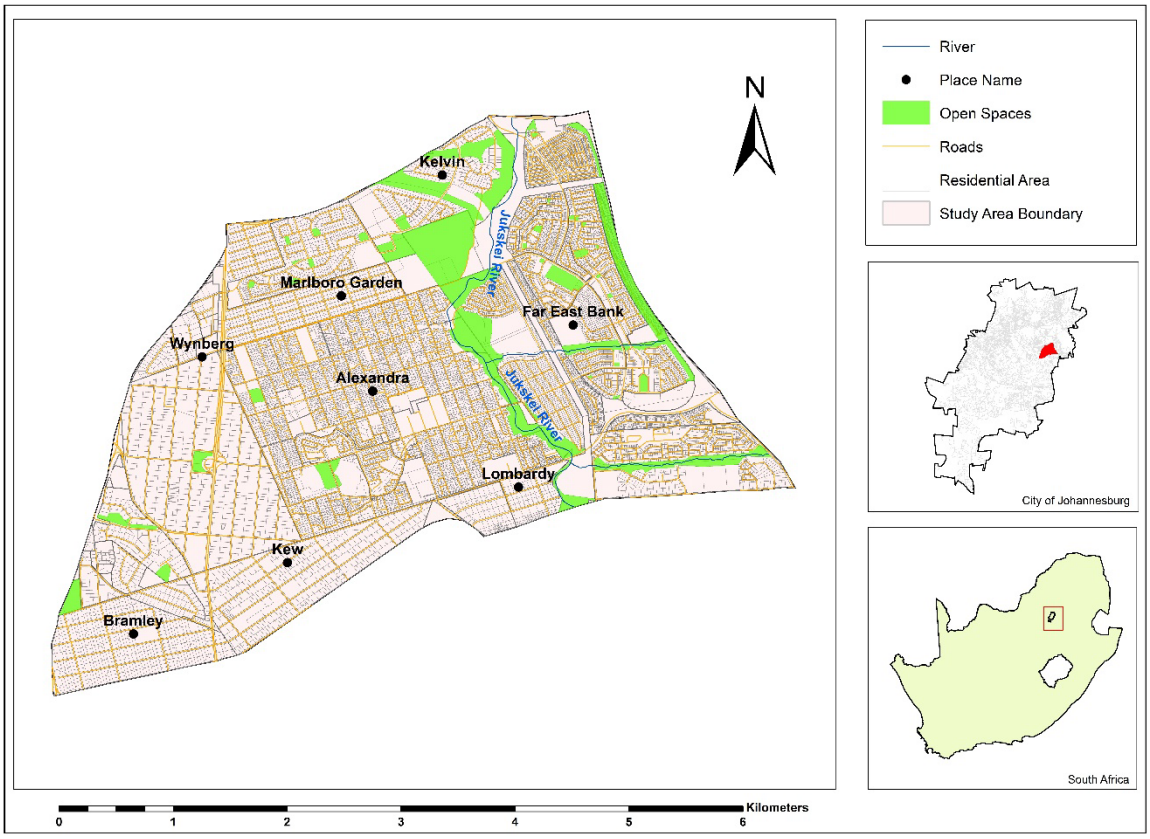

Figure 1: Location of the study area

$$Z_2 + Y_2 + a_2V_2^2 = \frac{Z_1}{2_g} + Y_1 + a_2V_1^2 + \frac{h_e}{2_g} \quad [1]$$

where:

Z_1, Z_2 = Elevation of the main channel inverts (m); Y_1, Y_2 = Depth of water at cross sections (m); V_1, V_2 = Average velocities (total discharge /total flow area); a_1, a_2 = velocity weighting coefficients; g = gravitational acceleration; h_e = energy head loss (m) which is calculated by the Manning formula as reported by Masoud (2016):

$$h_e = L\left(\frac{Q_n}{AR^{2/3}}\right)^2 \quad [2]$$

The Hydrologic Engineering Center-Geographic River Analysis System (HEC-GeoRAS) is a GIS interface tool used to capture the HEC-RAS geometric input data and to process its outputs, such as preparing flood maps based on water surface profile calculations (Ackerman, 2009). The HEC-GeoRAS can also handle output data created by HEC-RAS, thus allowing the import of predicted one- or two-dimensional water surfaces and velocity information back to the GIS for visualization and analysis. The HEC-GeoRAS has the capability of reading the HEC-RAS output file for further analysis, and mapping inundation as well as delineating floodplains (Ackerman, 2005).

4. Materials and methods

4.1. Datasets

Like any other modelling software, the HEC-GeoRAS and HEC-RAS have their own requirements, especially the amount of dataset input and the size of the area to be modelled. The datasets include both non-spatial (i.e., discharge data) and spatial data (i.e., LULC data and 2m DEM) that were used as the main data input into the model for creating RAS layers. In the present study, a maximum annual peak discharge data derived from the Soil and Water Assessment Tool rainfall-runoff modelling (SWAT) covering a period of 18 years (1993-2010) was used for flood frequency analysis and projecting discharge scenarios. The LULC information in the form of a map is one of the main required geometric layers in RAS geometry for deriving an attribute table containing Manning's '*N*-value' (i.e., roughness coefficient). Manning's '*N*-value' was used in the model to the define roughness of surfaces for each cross section. The classified LULC change maps for 1987, 2001 and 2015 derived from the Landsat satellite were used for this purpose. Manning's roughness coefficient '*N*-value' was assigned for each group of classified the LULC polygons using the method suggested by McCuen (1998) and Chow *et al.* (1988). Digital Elevation Models (DEMs) play a critical role in flood inundation mapping by providing floodplain topography as an input to hydrodynamic models, thereby enabling the mapping of the floodplain by using water surface elevations (Bates and De Roo, 2000; Casas *et al.,* 2006; Merwade *et al.,* 2008a). For the purpose of this study, a very high-resolution DEM (i.e., Spatial resolution of 2 m and 5 m vertical interval) covering the entire study area was acquired from the Centre for Geographical Analysis (CGA) at Stellenbosch University, South Africa (Van Niekerk, 2011).

4.2. Software

The software's that was used in this study was selected based on the capability to work on existing problems in an effort to achieve the study objective. In this study, Semi-Automatic Classification plug in Quantum-GIS was used for image pre-processing of Landsat images by applying the DOS1 atmospheric correction. The TerrSet Geospatial Monitoring and Modelling System was used for the image classification of the satellite images into LULC classes. ArcGIS 10.5 was used at different stages of the analysis of the geo-processing of satellite images and map generation. Previous methods used to delineate floodplain boundaries were primarily based on manual selection and required a considerable amount of time and effort (Noman *et al.,* 2001). With the development of numerical modelling, GIS and automated techniques become available and have been widely used in floodplain delineation. In this study, 1D HEC-RAS 5.0.3 and HEC-GeoRAS 10.5 were downloaded from the U.S. Army Corps of Engineers' website (http://www.hec.usace.army.mil/software/hec-ras/) for flood hazard mapping.

5. Methods used in research study

5.1. Pre-Processing Phase: Generating TIN and Geometric Layers

Digital Elevation Models (hereafter DEMs) play a critical role in flood inundation mapping by providing floodplain topography as input to hydrodynamic models thereby enabling the mapping of the floodplain by using water surface elevations (Bates and De Roo, 2000). For the purpose of this study, a very high-resolution DEM (i.e., Spatial resolution of 2 m and 5 m vertical interval) covering the entire study area was acquired from the Centre for Geographical Analysis (CGA) at Stellenbosch University, South Africa (Van Niekerk, 2011). In developing a floodplain delineation model, the first step in creating RAS layers, a 2 m DEM derived from LiDAR data was converted to a TIN using the 3D Spatial Analyst Tool in ArcMap. Figure 2 shows a TIN and geometric RAS layers required as input for HEC-RAS analysis.

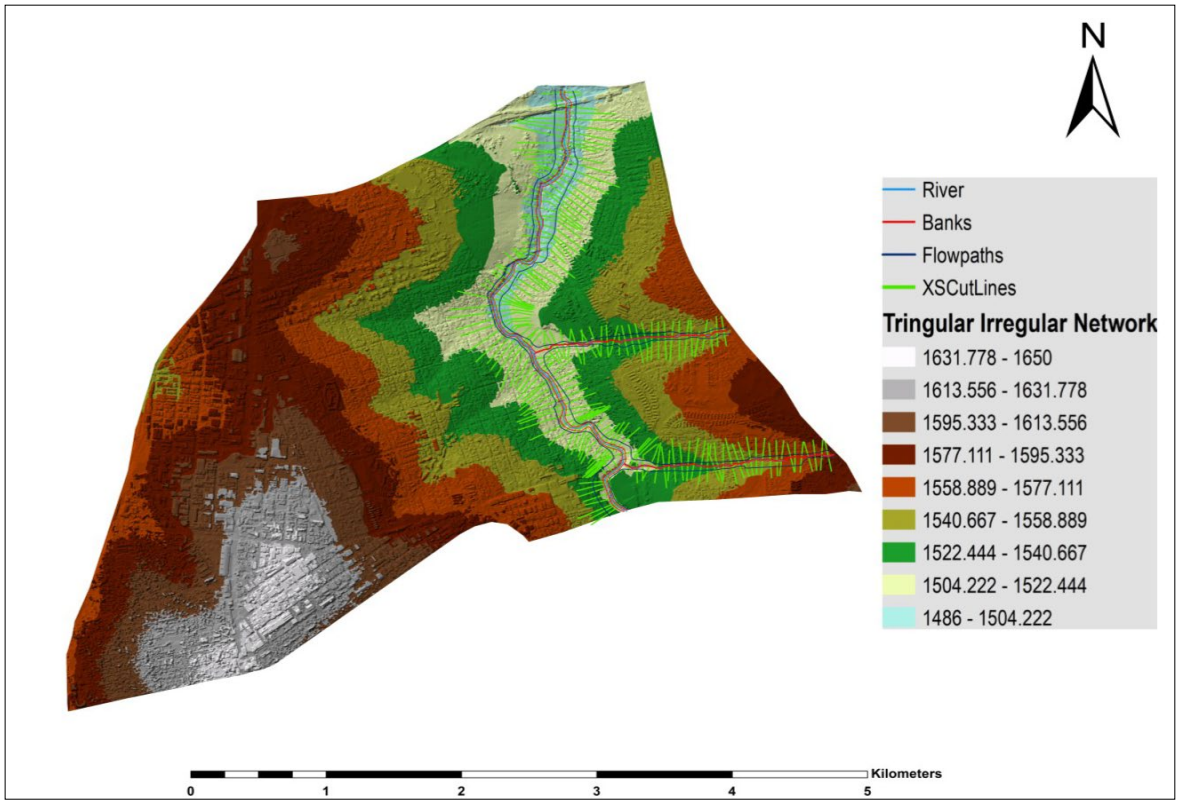

Figure 2: TIN and geometric RAS layers.

HEC-GeoRAS which contain RAS layers in a geo-database format has been used for geometric data development. Furthermore, A TIN was used in HEC-GeoRAS to create RAS layers which characterized the line and polygon themes (i.e., feature datasets). Figure 2 shows RAS geometry layers that are required for floodplain delineation. These include stream centrelines, flow paths, riverbanks and XS-Cutline (known as cross-section in HEC-RAS) and were captured in ArcMap using TIN and a geo-referenced Google Earth image. In the HEC-GeoRAS, each geometry layer and its attributes are stored in a separate feature class referred to as a RAS Layer (Merwade, 2009). All these layers were then imported into the HEC-RAS 5.0 for post-processing and model development.

5.2. LULC Map and Manning's Coefficient "N-Value"

In this study, multi-temporal classified Landsat satellite images of the 1987 Multi-Spectral Scanner (hereafter MSS) and the 2015 Operational Land Imager (hereafter (OLI) were used interchangeably to assess the hydrological change in the floodplain due to a change in the LULC (i.e., built-up area, bare surface, intact vegetation and sparse vegetation). In the HEC-GeoRAS, these datasets must be in a vector format with a field named "*N*-value", where Manning's coefficient value for each cross-section XS-cutlines will be extracted (Ackerman, 2005; Hernandes and Zhang, 2007; Merwade, 2009). Moreover, as Chow (1959) mentioned, hydraulic calculations of the flow in channels and overbank areas of floodplains require an evaluation of roughness characteristics. Therefore, selecting appropriate Manning's *N*-values is very important for accurate computation of water surface profiles. For the purpose of this study, the Manning's *N*-values were adapted from Chow (1959) after Chow *et al.* (1988) and Selby, (1988) and were assigned to each classified LULC class. Table 1 represents the Manning's *N*-values that were used in this study and the Manning's *N*-values in HEC-RAS extracted from LULC.

Table 1: Manning's coefficient value for LULC classes (Source: Chow, 1959; Selby, 1988).

LULC type	Manning's *N*-value	LULC Description
1. Bare surface	0,005	This describes the area without vegetation cover.
2. Built-up area	0,200	This category includes areas with high density of residential area and roads.
3. Intact vegetation	0,085	Area covered with dense vegetation, land allocated for agricultural lands and natural landscaping.
4. Sparse vegetation	0,050	Areas with very little vegetation cover, they consist of areas with scattered vegetation, areas with a cover of shrubs and short trees mixed with grasses.

5.3. Flood Frequency Analysis using Log-Normal Distribution

In the present study, a maximum annual peak discharge data derived from SWAT rainfall-runoff modelling covering a period of 18 years (1993-2010) was used for flood frequency analysis and projecting discharge scenarios (see Table 2). SWAT is a highly data sensitive semi-distributed model that requires specific geographic information data about the catchment characteristics. These includes DEM, LULC, soil data and its properties, climate data and peak discharge data in a raster format. The SWAT model was calibrated for 10 years (1993-2003) and 6 years for the validation (2004-2010). Four statistical methods were used to evaluate SWAT model performance (i.e., N_{SE}, R^2, RSR, and PBIAS) by comparing observed direct runoff with SWAT simulated runoff. The objective function during calibration was specified as NSE > 0,5 in SUFI-2; thus, 0,72 and 0,68 for N_{SE}; 0,84 and 0,68 for R^2; 0,54 and 0,63 for RSR; and 16,5 and 20,4 for PBIAS during model calibration and validation, respectively (Mawasha and Britz, 2020). These datasets were further analysed and ranked by assigning a rank of one to the largest peak discharge and eighteen to the smallest peak discharge.

From these rankings, the recurrence intervals were calculated using the following equation (Baer, 2008; Görgens, 2003):

$$T = (n + 1) / m \quad [3]$$

where:

T represents the recurrence interval (in years) for each flood, *n* is the number of annual flood peak discharge, m shows the rank of flood; the highest peak has *m* = 1, second highest peak has *m* = 2, and so on (Kiely, 1998). A flood frequency analysis was performed where the recurrence interval was transformed into logarithm form (base 10). The recurrence interval and peak discharge were further plotted on a flood frequency graph using a Log-Normal distribution where the vertical (*y*) and horizontal (*x*) axes represent the peak discharge and flood return period, respectively (see Table 6.2 and Figure 6.9a-c). In this study, three profiles were selected, that is, a 2-year, 25-year and 100-year flood return period, which was used to estimate the associated peak discharge for delineating floodplains for each year. The following logarithm equations were used in this study to estimate peak discharge for flood return periods of 1987and 2015 LULC, respectively:

$$y = 716.0\text{In}(x) - 215.4 \quad [4]$$

$$y = 1164.2\text{In}(x) - 86.3 \quad [5]$$

where:

y represents the peak discharge (m3/s) and x represents flood return period (years).

Table 2: Peak discharge derived from SWAT model for different LULC conditions**.**

Date	Rank (m)	1987 LULC	2001 LULC	T = n + 1\m
		Discharge (m^3/s)	Discharge (m^3/s)	
2009 – January	1	1850,13	2320,89	19,00
1997 – March	2	1515,38	2200,58	9,50
2008 – January	3	1416,09	2072,26	6,33
1996 – February	4	1011,65	1394,30	4,75
2000 – March	5	550,35	1106,25	3,80
2006 – January	6	416,47	1077,78	3,17
2010-January	7	401,42	889,76	2,71
2007 - October	8	290,95	589,15	2,38
1995 – December	9	138,07	362,39	2,11
2005 – April	10	137,58	306,45	1,90
1998 – October	11	90,02	297,38	1,73
2001 – May	12	47,42	174,27	1,58
1993 – November	13	37,32	144,57	1,46
2004 – March	14	36,87	140,58	1,36
2003 – October	15	35,12	139,57	1,27
2002 – August	16	15,46	59,92	1,19
1994 – February	17	13,45	52,12	1,12
1999 – October	18	8,64	33,48	1,06
	n = 18	**Average = 445,13**	**Average = 742,32**	

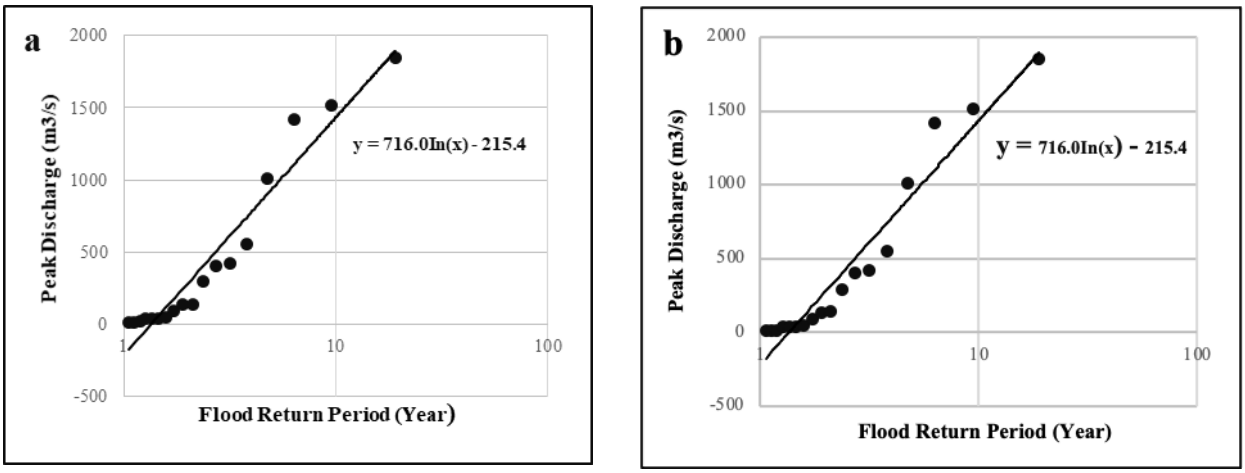

Figure 6.9: Log-Normal distribution graph used for estimating peak discharge for flood return period: (a) 1987 and (b) 2015.

5.4. Post-Processing of Geometric Data

Once the cross-sections XS-cutlines are populated using TIN, the entire input datasets, including the stream centreline, banks, flow paths, and Manning's *N*-values were exported into HEC-RAS for further hydraulic analysis. This procedure allows the geometric data to be transferred from HEC-GeoRAS to HEC-RAS format for a flood simulation model. The portion of the Jukskei River that flows through Alexandra Township was assumed to have a steady flow. Steady flow rivers can be defined as rivers which assumed to flow steadily along the reach as the energy equation is not time dependent (Salimi *et al.,* 2008). RAS geometric layers that were generated using RAS geometry were further exported to be processed and analysed in HEC-RAS 5.0.3. Data requirements such as boundary conditions, peak flow and cross-sections, were analysed in order to execute the HEC-RAS model. Boundary conditions are necessary to establish the starting water surface at the ending of the river system. A starting water surface is necessary in order for the programme to begin the calculations. The Jukskei River profile from the upstream to downstream catchment was calculated using a TIN and was further used as the model's initial boundary condition (normal depth) for the steady flow. In this research, normal depth was selected for upstream boundary conditions and critical depth was selected for downstream boundary conditions. Peak discharge for 2, 25 and 100-years return periods were estimated using the Log-Person Type III distribution flood frequency analysis using peak discharge data derived from the SWAT model (Mawasha and Britz, 2020). The HEC-RAS consists of three flow regimes (i.e., subcritical, supercritical and mixed flow regimes) which are used in modelling a network of channels and river reaches (Chaudhry, 2011; Morche *et al.,* 2010; Tate *et al.,* 1999). In this study a steady flow analysis was performed using a mixed flow regime. Lastly, the RAS mapping was used for simulating water surface generation, flow velocity and floodplain delineation, whereby TIN elevations were subtracted from simulated water surface elevations to get a spatial extent of flood inundation and flood depth (Noman *et al.,* 2001).

5.5. Validation of the HEC-RAS model

Validation requires that predictions of a model are compared to observed data in order to demonstrate the accuracy and reliability of the model (Grimaldi *et al.*, 2016). In order to avoid misleading conclusions, Mason *et al.* (2009) and Di Baldassarre, Schumann and Bates (2009) recognized the need for testing the model results for both precision and accuracy. Several studies have utilized RS data, such as that collected from Landsat-MSS and TM/Enhanced Thematic Mapper Plus (ETM+), Advanced Very High-Resolution Radiometer (AVHRR) and Moderate Resolution Imaging Spectroradiometer (MODIS) to determine the extent of floodplain inundation (Huang, Chen & Wu, 2014; Chen et al., 2013; Townsend & Walsh, 1998). However, the timing of capturing flooded areas during rainfall is the main limitation in the use of satellite remote sensing data to validate flood simulation derived from HEC-GeoRAS and HEC-RAS. Therefore, due to the fact that a satellite might only revisit an area of interest every sixteen days, major flood events that occurred in the study area (i.e., 2000, 2009, 2010, 2015 and 2016) were not captured by satellite images. Nevertheless, the available satellite images that were taken during a flood event and two to three days after the flood event in the study area for validation, were covered by clouds which limits the detection of floodwater. Therefore, the model validation for this study was conducted by conducting a fieldwork, and with the help of residents by taking measurements of the previous flood extent and depth and proximity of buildings to the riverbank.

6. Results and discussion

6.1. Change in LULC

In this study, to evaluate LULC changes for the past 28 years and to see how the location of these changes affect flow characteristics, historic and current LULC conditions were considered. LULC classes considered for the analysis in this study are bare surface, built-up area, intact vegetation and sparse vegetation. The resulting LULC maps generated for the study area for the year 1987 and 2015 are presented in Figure 3. Table 2 shows the statistical variation in LULC under each category of LULC between the year 1987 and 2015. The analysis of the results revealed that there has been increase in built-up area by 22%, reduction in intact and sparse vegetation by 8,4% and 15,6%, respectively for the last 28 years. With reference to the study analysis and results, it can be concluded that there is substantial LULC change as compared to natural land cover that existed in the year 1987 and rapid urbanisation that the study area has undergone for the last 28-years.

Table 2: Land use/land cover changes for the study area with changes from 1987 to 2015.

LULC classes	1987 LULC (ha)	2015 LULC (ha)	% Change
Bare Surface	20,0	43,8	+ 1,6
Built-up Area	934,2	1277,2	+ 22,5
Intact Vegetation	190,5	62,4	– 8,4
Sparse Vegetation	380,8	142,1	– 15,6

Figure 3: Land use/land cover maps (a) for the year 1987 and (b) for the year 2015.

6.2. Flood Depth Change due to LULC Change

Figure 4 (a) to (c) and Figure 5 (a) to (c) shows the flood depth maps for 2, 25, and 100-year flood return periods for 1987 and 2015 LULC conditions. The analysis of the results revealed that, the depth at the stream centreline is higher compared to areas alongside the stream centreline with varying flood depths. According to Emergency Management Australia (1999) wading by an able-bodied adult person becomes more difficult and dangerous when the depth of still water exceeds 1,2 m and light vehicles can become unstable when the water depth exceeds 0,3–0,4 m. The results of the model simulation using HEC-GeoRAS showed that there is an increase in flood depth for 2, 25 and 100-year return periods due to LULC change. For example, during 1987 LULC conditions, an average flood depth was 1,3 m with a maximum flood depth of 2,3 m while during 2015 LULC conditions an average flood depth 1,9 m with maximum flood depths of 3,0 m were reached for some areas along the river. Thus, for the past 28-years (i.e., 1987 to 2015) the maximum flood depth increased by 0,7 m, thereby increasing the risk of infrastructure and residence along the Jukskei River to flash floods.

6.3. Effect of LULC Change to Flow Velocity

The flow velocity is a component of flood water that can make objects like cars and houses float and can sweep people away. The flow velocity maps for different return periods for different LULC conditions are shown in Figure 6 and Figure 7. Cao *et al.* (2013) asserted that sliding instability

usually occurred when the flow velocity is less than 0,25 m/s, while toppling instability generally occurred when flow velocity is greater than 2,5 m/s.

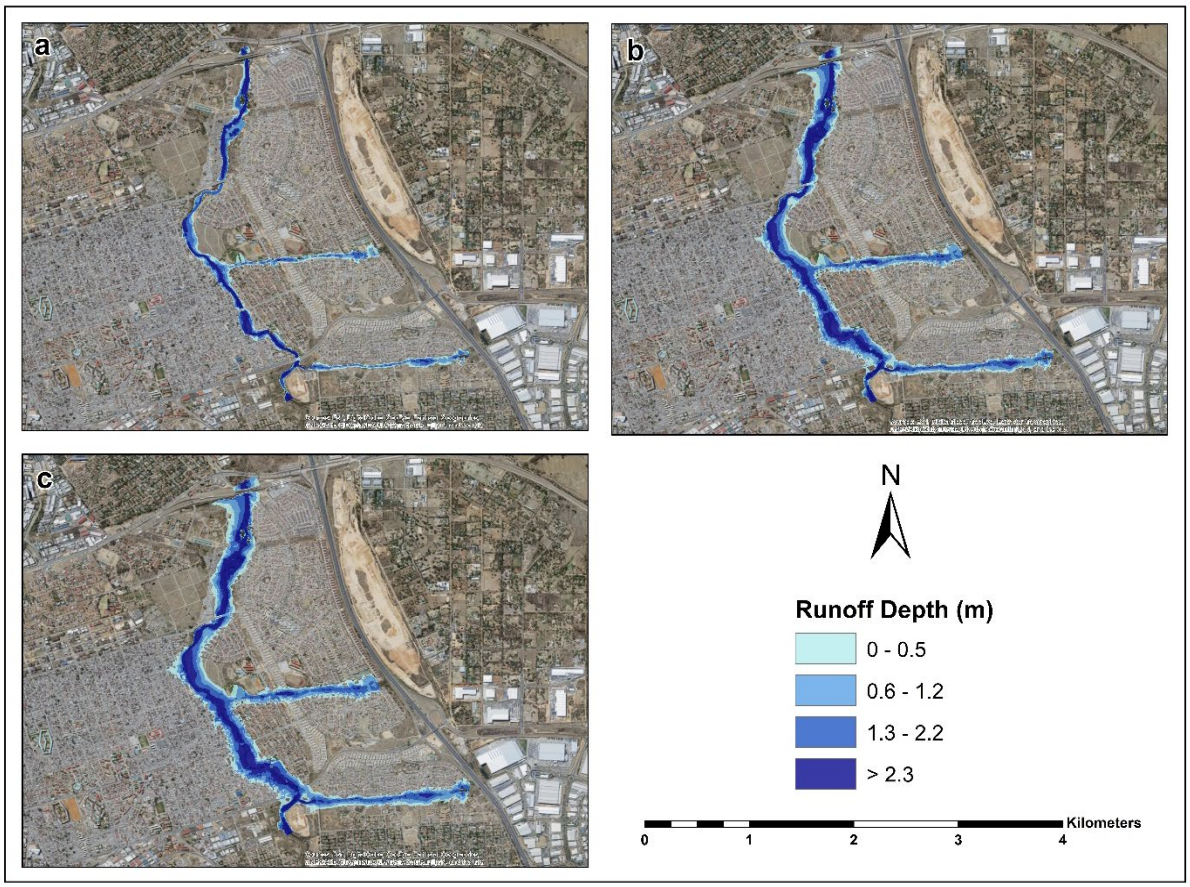

Figure 4: Flood depth maps for LULC of 1987 (a) 2; (b) 25 and (c) 100-year flood return.

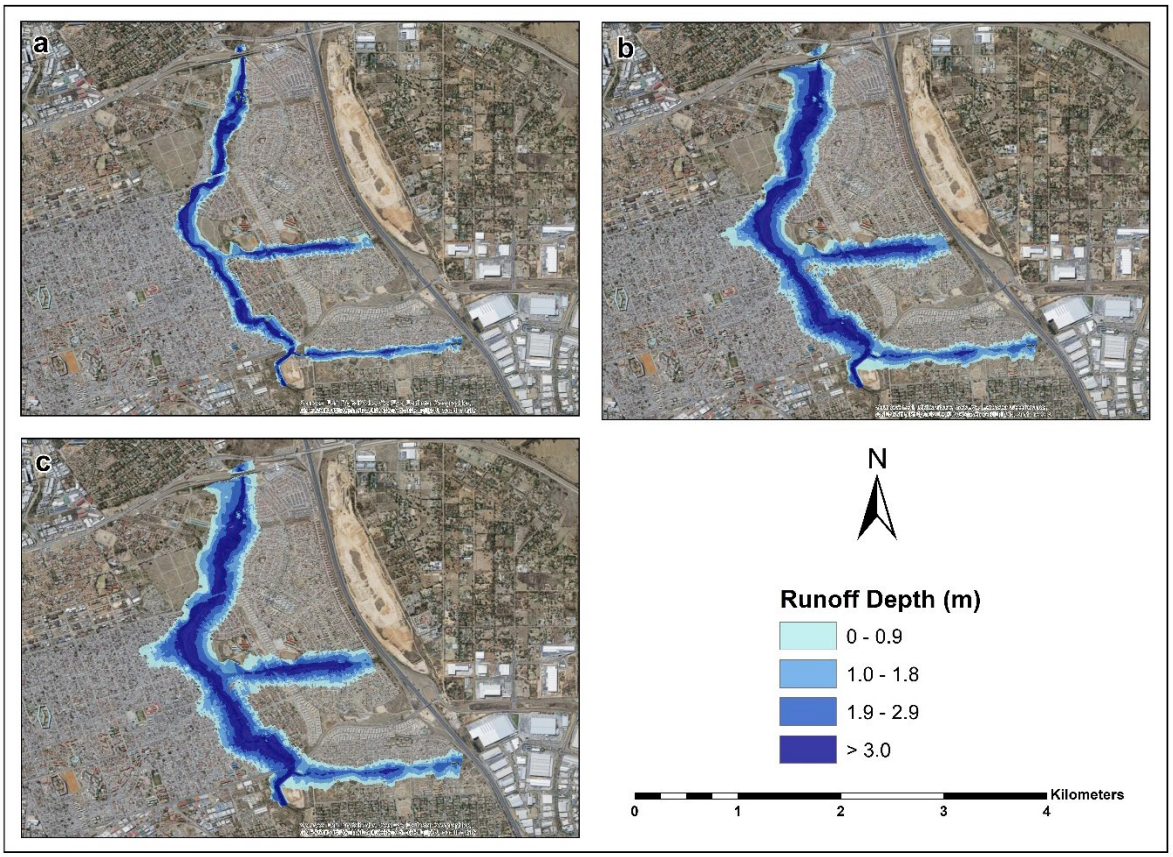

Figure 5: Flood depth maps for LULC of 2015 (a) 2; (b) 25 and (c) 100-year return periods.

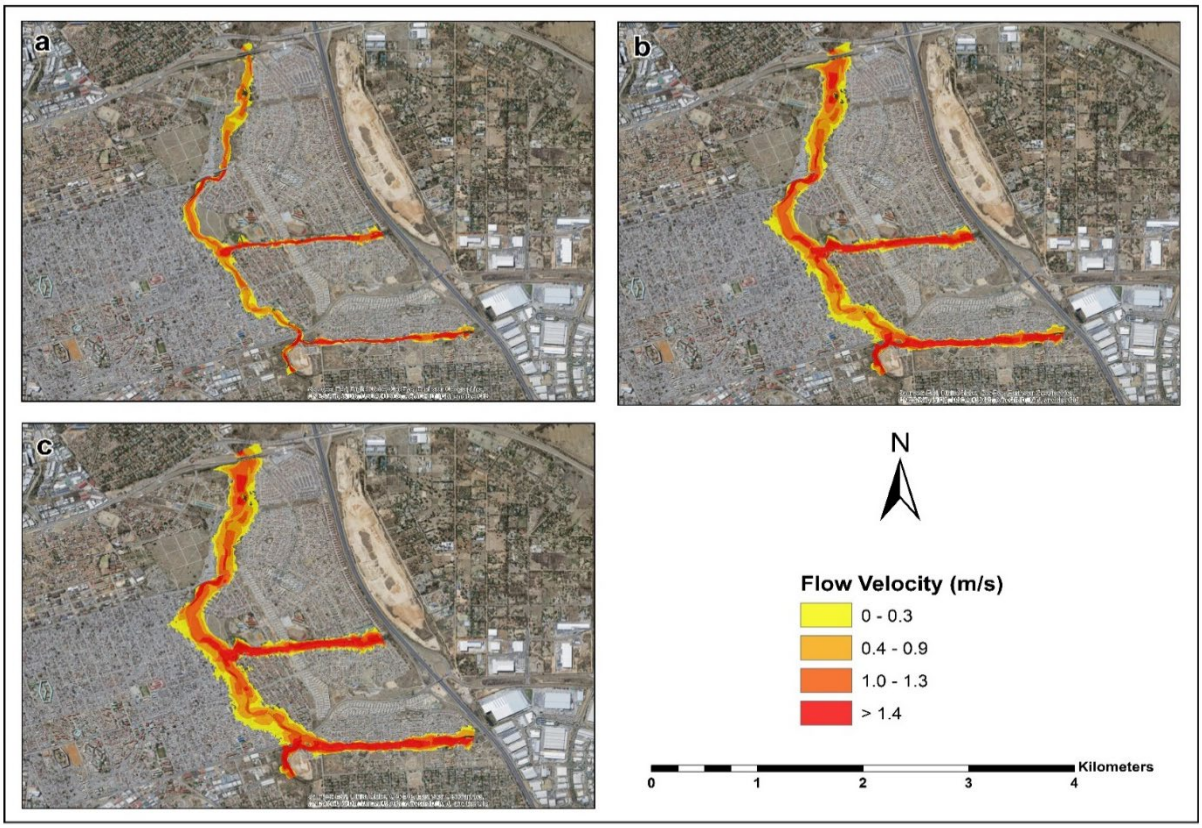

Figure 6: Flow velocity map for 1987 LULC (a) 2, (b) 25 and (c) 100-year return periods.

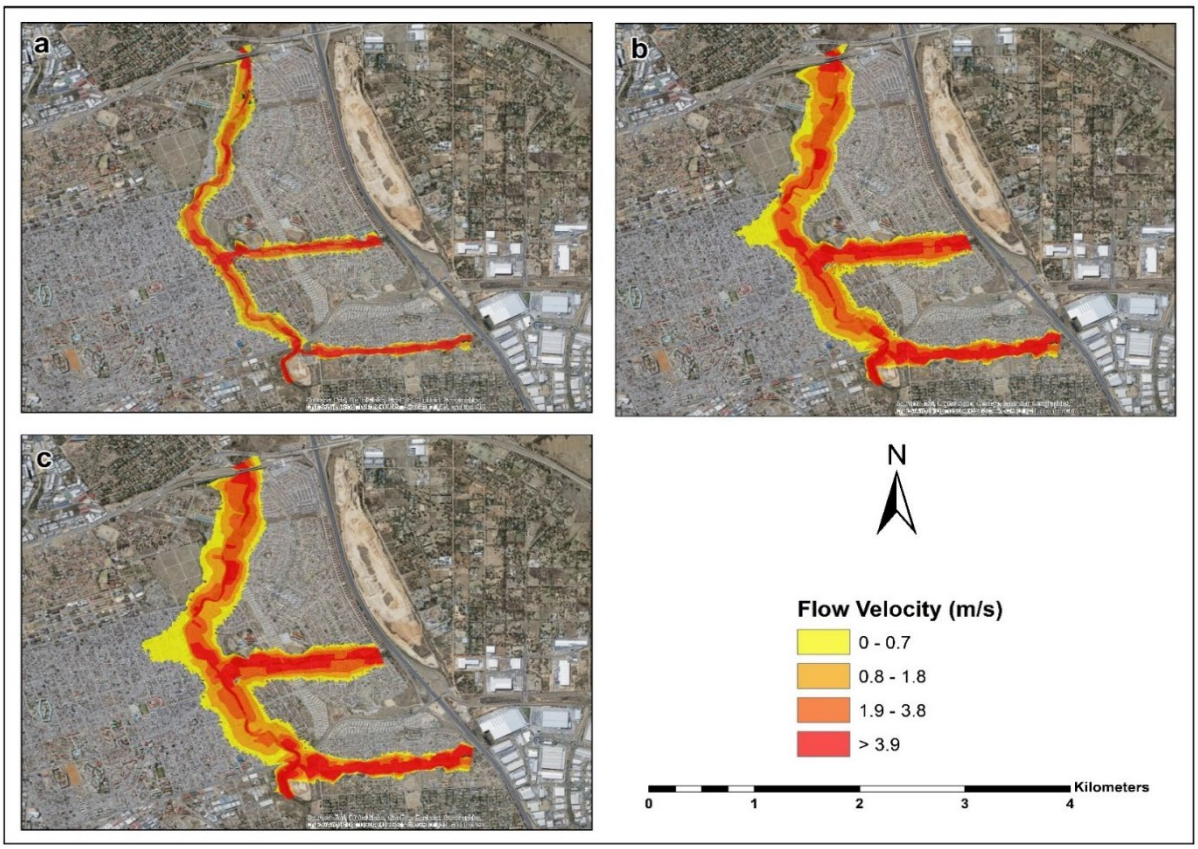

Figure 7: Flow velocity maps for 2015 LULC (a) 2, (b) 25 and (c) 100-year return periods.

According to Marco (1994) cited by (Merz *et al.,* 2007) a person may be swept away when the velocity is above 0,5 m/s. The study simulated flow velocity were found to be greater than the flow velocity suggested by Cao *et al.* (2013) during the 2015 and 1987 LULC simulation with a maximum flow velocity of 3,9 m/s and 1,4 m/s which will enable individuals to topple or slide that can lead to drowning and consequently to loss of life, serious injuries and the floating of cars, depending on the size of the vehicle.

6.4. The Effect of LULC Change to Flood Depth-Velocity Change

Flow velocity alone cannot estimate the potential damage due to flash floods, but when combined with flood depth it can be used to predict the areas that are prone to flash floods. Prediction of flood depth and flow velocity is particularly important when predicting the risk of flash floods (Asano and Uchida, 2016). Therefore, in this study a depth-velocity combination method was adopted and applied to analyse the effect of flash floods (i.e., hazard level) to communities and infrastructure along the Jukskei River and its tributaries (Clausen, 1989). The combination of maximum flood depth (d-[m]) and maximum flow velocity (v-[m/s]) is represented in this study as dv (depth-velocity) with unit [m^2/s]. Figure 8 to Figure 9 show spatial distribution of the flood depth-velocity product used in this study for 1987 and 2015 LULC for 2-year, 25-year and 100-year flood return periods. The analysis of the results revealed that there was an increase in depth-velocity from 2,9 m^2/s to 6,3 m^2/s with an average of 1,7 m^2/s and 3,5 m^2/s for the 1987 and 2015 LULC conditions, respectively. Jonkman

(2009) performed an experimental test on individual and vehicle instability done in Japan. The experiment showed that people may experience difficulties in walking through water when the depth-velocity product exceeds 0,5 m^2/s and cars may lose stability when depth-velocity the product exceeds 1,0 m^2/s depending on the size of the car. Experimental studies found that people become unstable in water when depth-velocity product ranges from 0,6 m^2/s to about 2,0 m^2/s (Lind *et al.,* 2004; Jonkman, 2009).

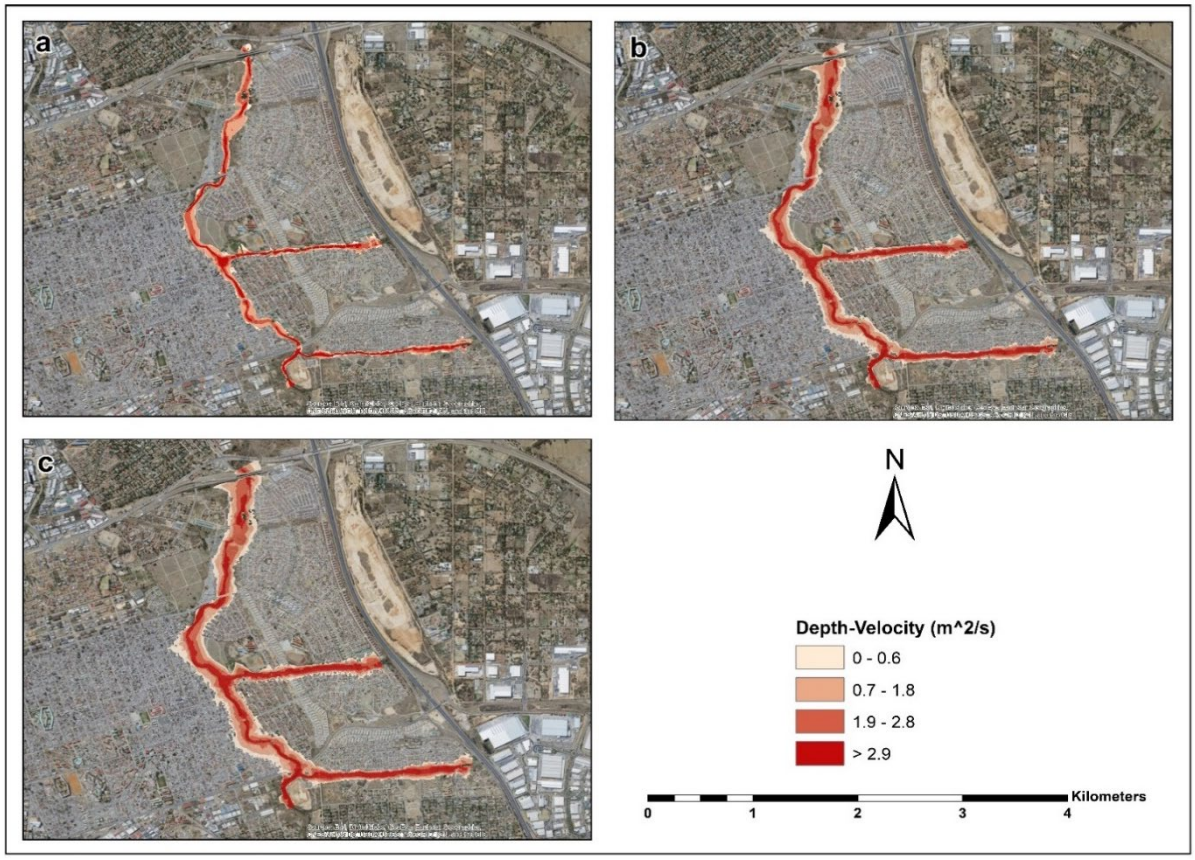

Figure 8: Depth-flow velocity for 1987 LULC (a) 2, (b) 25 and (c) 100-year return period.

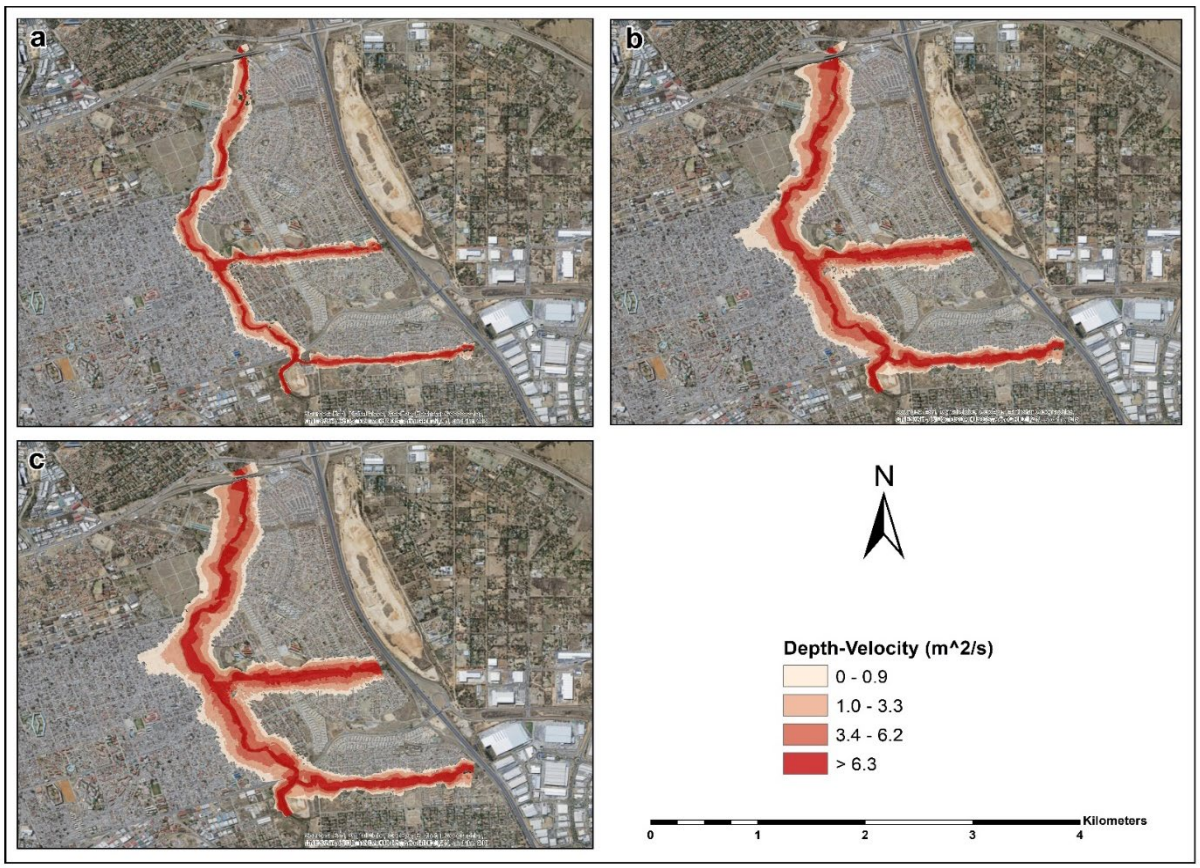

Figure 9: Depth-flow velocity for 2015 LULC (a) 2, (b) 25 and (c) 100-year return period.

With that being said, the minimum, average and maximum depth-velocity values of the study (i.e. 0,6 m^2/s, 1,7 m^2/s and 2,9 m^2/s for 1987 LULC and 0,9 m^2/s, 3,5 m^2/s and 6,3 m^2/s for 2015 LULC) were far higher in comparison to those suggested by the Federal Emergency Management Agency (1979), Abt *et al.* (1989), Suetsugi (1998), Lind *et al.* (2004) and Jonkman (2009), which indicates that people's instability, infrastructure, residential properties (i.e. types of material used) and livestock's within the depth-velocity ranges will be at risk of being affected by flash floods during intense rainfall. Moreover, based on modelled depth-velocity comparison with the Jonkman and Penning-Roswell (2008) studies, individuals will topple or slide, depending on their gender, age, height, weight and disability. However, with reference to 2015 LULC conditions and the drainage system within the catchment area, during intense rainfall light constructed houses along the Jukskei River, cars and humans, including adults, individuals with disabilities and children are at risk of instability due to high depth-velocity of flood water. During 1987 LULC the impact of flooding was minimal compared to 2001 and 2015 LULC where high flood depth, flow velocity and depth-velocity covered a large area and reached to residential areas where it could cause instability of individuals, cars/vehicles and cause damage to buildings. This is aggravated by tremendous change in the LULC within the study area where natural land cover was replaced by an impervious surface which limits rainfall infiltration rate into the soil, thereby increasing surface runoff depth and velocity.

7. Analysis of field observations

Due to the unavailability of reference data i.e., satellite images captured during flood incidence to validate the HEC-RAS modelling output results, field work and observations were conducted in the study area during the dry season in an effort to assess the impact of previous floods and contributing factors that worsen flood impact along the Jukskei River. Fordham, Tunstall & Penning-Rowsell (1991) suggest the probability of flooding is higher for those living on the banks of the river. Along the Jukskei River, the horizontal distance of the building to the edge of the river channel varies, as some buildings are located at the edge of the river channel while others range from 1 m to more than 20 m (see Figure 10) from the riverbank. With reference to Figure 7.5, the majority of buildings are located within the floodplain areas where floodwater from the Jukskei River will overflow into the homestead during intense rainfall. Moreover, during severe flash floods, the river channel adjusts its morphology (i.e., channel width and depth) to accommodate high surface runoff, which causes landslides and thus increases the risk of flooding in buildings near the river channel.

As shown in Figure 10, above, the buildings are closely located to each other at close proximity to the Jukskei River. During the 9 November 2016 Gauteng flash floods (flood victims' communication), the floodwater level of more than 1,5 m above the ground surface reached these buildings. Satterthwaite *et al.* (2007) note that certain areas in the developing countries don't have adequate roads, residents live in inferior homes and even unlawfully occupied land. This is the case especially in areas along the Jukskei River, as shown in Figure 10 (c). Through the researcher's observation, the materials (i.e., non-durable materials) used to construct these buildings and their distance to the Jukskei River increases their vulnerability to the impact of flash floods; this will cause loss of property, human lives and livelihoods. As reported by Adelekan (2011), people living within 500 m from the river can experience higher economic losses and human death due to the consequences of more extreme and severe flooding, though people living more than 1 km from the river are not subject to flood disasters.

The vertical and horizontal distance of the buildings to the riverbanks are critical indices for the evaluation of residential building vulnerability during flash floods (Du, He, Wang, Zhang & Li, 2015). Figure 11 below, illustrates the depth of previous flood water levels in affected areas, with the help of affected flood victims. Most of the properties that were surveyed during the field work are located at different distances from the river, that is, less than 30 m from the stream centreline with different elevation levels. In Hue District, central Vietnam, a study revealed that poor households had flooding in their homes at rates greater than 40 cm than rich households with houses constructed at higher-level (Tran *et al.*, 2008). During the field work, it was observed that the lowest flood-water level (i.e., vertical distance from the ground surface) measured was 0,4 m, 0,8 m and 1,2 m (see Figure 11) with a horizontal distance of 28,6 m, 9 m and 5,4 m, respectively, from the stream- centreline. Due to the characteristics of the area along the Jukskei River, and human activities, it can be suggested that the minimum safe vertical distance of buildings should have at least 0,5 m up to 1 m above the ground surface level. While the horizontal distance should be more than 100 m from the river edge. This is the least that must be maintained in order to minimize the susceptibility of flooding impacts

along the Jukskei River. However, the presence of a bridge across a river can have a negative influence on hydrology (Blanton & Marcus, 2009). In relation to the results of the HEC-RAS production model, the water level is high near the bridge, resulting in backwater, aerial flooding extent, and flooding concentration time in nearby areas. Figure 12, below, shows one of the analysed bridges with a height of 3,2 m and a width of 16 m. In the middle section of the river where this bridge is located high discharge normally occurs. During intense rainfall, the bridge is frequently flooded, which makes it impossible for the area to be accessed. In addition, the depth-velocity of flooding near this bridge is high, as shown by the debris mounted on the pier reaching the top of the bridge. With that being said, the bridge is improperly designed in that its height is on the same level as the earth's surface. Moreover, at the bridge, the river is narrowed and not deep enough to accommodate high surface runoff volume.

Figure 10: Proximity of residential buildings from the riverbank

Figure 11: Historic flood water level above ground in various locations along the Jukskei River

Figure 12: Photographs of a bridge (a) during the normal period and (b) during the rainy season

8. Conclusion

Change in the LULC over time due to residential, administrative and infrastructure development to satisfy the population's needs has led to rapid LULC change where natural land cover is replaced by impervious surfaces. Alexandra Township faces a scarcity of land and has limitations for development. As a result, individuals are residing in areas declared as flood-prone areas along the

Jukskei River. Flooding, especially along Jukskei River, is known as the most frequent phenomenon that has occurred every year as a result of intense rainfall and other contributing factors. In this study, the effect of LULC change on flooding have been investigated for Alexandra Township along the Jukskei River and its tributaries by considering the changes for 28 years. The integration approach of hydraulic and hydrological models of the HEC-RAS and HEC-GeoRAS with the GIS and remote sensing techniques has been used for flood plain modelling. The LULC analysis of Alexandra Township showed 22,5% increase in built-up area and 8,4% and 15,6% reduction in intact vegetation and sparse vegetation respectively. Thus, there have been temporal and spatial changes in the LULC for the last 28 years (between 1987 and 2015). The results obtained from the present study revealed that there is a change in flood hazard extent due to change in the LULC. The analysis of the HEC-RAS/HEC-GeoRAS model output revealed that flood depth increased from 2,3 m to 3,0 m, flow velocity increased from 1,4 m/s to 3,9 m/s and depth-velocity increased from 2,9 m^2/s to 6,3 m^2/s for 1987 and 2015 LULC conditions respectively. The flood hazard maps developed in this study can be useful to the municipality and private organisations for flood mitigation, management and preparedness for planning and an early evacuation management plan during flood events. Additionally, these maps will be also useful to insurance companies to decide on the criteria to set premiums for residential and administrative structures located in the flood zone area.

References

Abt, S.R., Wittler, R.J., Taylor, & Love, D.J. (1989). Human stability in a high flood hazard zone. *Water Resource Bulletin*, 25(4), 881-890.

Ackerman, C.T. (2005). HEC-GeoRAS, GIS tools for support of HEC-RAS using ArcGIS. Davis: United States Army Corps of Engineers.

Ahmad, B., Muhammad, S.K., Butt, M.J., & Dahri Z.H. (2010). Hydrological modeling and flood hazard mapping of Nullah Lai. *Proceedings of the Pakistan Academy of Sciences* 47(4), 215–226.

Ali, M., Khan, J., Aslam, I., & Khan, Z. (2011). Simulation of the impacts of land use change on surface runoff of Lai Nullah basin in Islamabad, Pakistan. *Landscape and Urban Planning*, 102, 271–279.

Al-Rawas, G.A., Valeo, C., Khan, U.T., & Al-Hafeedh, O.A. (2015). 'Effects of urban form on wadi flow frequency analysis in the Wadi Aday watershed in Muscat, Oman'. *Urban Water Journal*, 12(4), 263–274.

Asano, Y., & Uchida. T. (2016). Detailed documentation of dynamic changes in flow depth and surface velocity during a large flood in a steep mountain stream. *Journal of Hydrology*, 541, 127–135.

Bates, P.D., & De Roo, A.P.J. (2000). A simple raster-based model for flood inundation simulation. *Journal of Hydrology*, 236, 54–77.

Cao, L., W, Zhong, G.H., Liu, S.G., & Wu, X.G. (2013). Analysis of human instability in flood flow. *Journal of Tongji University (Natural Science),* 41(11), 1675-81.

Casas, A., Benito, G., Thorndycraft, V.R., & Rico, M. (2006). The topographic data source of digital terrain models as a key element in the accuracy of hydraulic flood modelling. *Earth Surface Processes and Landforms,* 31(4), 444–456.

Chaudhry, M.H. (2011). Modeling of one-dimensional, unsteady, free-surface, and pressurized flows. *Journal of Hydraulic Engineering,* 137(2).

Chow, V.T. (1959). Open Channel Hydraulics, New York, McGraw-Hill, 680.

Chow, V.T., Maidment, D.R., & Mays, L.W. (1988). Applied hydrology, McGraw- Hill, New York.

City of Johannesburg (2008). State of environment Report for 2008. Johannesburg, Braamfontein.

Clark, M.J. (1998). Putting water in its place: A perspective on GIS in hydrology and water management. *Journal of Hydrological Process,* 12, 823–834.

Clausen, L.K. (1989). Potential dam failure: estimation of consequences, and implications for planning. Unpublished M.Phil. Thesis at the School of Geography and Planning at Middlesex Polytechnic collaborating with Binnie and Partners, Redhill.

Dewan, A.M., & Yamaguchi, Y. (2009). Land use and land cover change in Greater Dhaka, Bangladesh: using remote sensing to promote sustainable urbanization. *Applied Geography*, 29, 390–401.

Dyhouse, G., Hatchett, J., Benn, J., & Methods, H. (2003). Floodplain Modeling using HEC-RAS. Waterbury, CT, Haestad Press.

Emergency Management Australia (1999). Managing the Floodplain - Manual 19. Australian Emergency Manuals Series, Emergency Management Australia, Attorney General's Department, Australian Government.

Federal Emergency Management Agency (1979). Federal Guidelines for Dam Safety. Federal Emergency Management Agency.

Fosu, C., Forkuo, E., & Asare, M. (2013). "River inundation and hazard mapping- A case study of Susan River-Kumasi". Proceedings of Global Geospatial Conference, Qubec City, Canada, 14–17.

Hausmann, P., & Weber, M. (1988). Possible contributions of hydro informatics to risk analysis in insurance, In: Proc. 2nd International Conference on Hydro informatics, Zurich, Switzerland, 9– 13 September, Balkema, Rotterdam. Hydrologic Engineering Center.

Hernandes, T., & Zhang, P.E. (2007). Floodplain analysis using computational tools. Paper presented at the World Environmental and Water Resources Congress of the Environmental and Water Resources Institute, Tampa.

Hydrologic Engineering Center, (2005). HEC-RAS river analysis system. Hydraulic Reference Manual ver. 3.1.3 US. Army Corps of Engineering.

Jonkman, S.N. (2009). Human Instability in Flood Flows 1, 44(4), 1-11.

Jonkman, S.N., & Penning-Rowsell, E. (2008). Human instability in flood flows. *Journal of the American Water Resources Association*, 44(4), 1–11.

Lastra, J., Fernandez, E., Diez-Herrero, A., & Marquinez, J. (2008). Flood hazard delineation combining geomorphological and hydrological methods: an example in the Northern Iberian Peninsula. *Natural Hazards*, 45, 277–293.

Lind, N., Hartford, D., & Assaf, H. (2004). Hydrodynamic Models of Human Stability in a Flood. *Journal of the American Water Resources Association (JAWRA)*, 40(1), 89-96.

Lugeri, N., Kundzewicz, Z.W., Genovese, E., Hochrainer, S., & Radziejewski, M. (2010) River flood risk and adaptation in Europe-assessment of the present status. *Mitigation Adaptation Strategy and Global Change*, 15, 621–639

Masoud, M.H., (2016). Geo-informatics application for assessing the morphometric characteristics' effect on hydrological response at watershed (case study of Wadi Qanunah, Saudi Arabia). *Arabian Journal of Geosciences*, 9, 280.

McCuen, R.H. (1998). Hydrologic analysis and design, Prentice-Hall, New Jersey.

Merwade, V. (2009). Tutorial on using Hec-GeoRAS with ArcGIS 9.3 [online].

Merwade, V., Cook, A., & Coonrod, J. (2008a). GIS techniques for creating river terrain models for hydrodynamic modeling and flood inundation mapping. *Journal of Environmental Modelling and Software*, 23, 1300–1311.

Merz, B., Thieken, A.H., & Gocht, M. (2007). Flood risk mapping at the local scale: concepts and challenges. In: Begum S, Stive M, Hall J (eds) Advances in natural and technological hazards research. Springer, Dordrecht, 231–251.

Morche, D., Rascher, E., Bimböse, M., Nicolay, A., & Schmidt, K.H. (2010). Modeling sediment transport in an alpine river reach with HEC-RAS 4.0.

Mucina, L., & Rutherford, M.C. (2006). The Vegetation Map of South Africa, Lesotho and Swaziland. SANBI, Pretoria.

Noman, N., Nelson, J., & Zundel, A. (2001). Review of automated floodplain delineation from digital terrain models. *Journal of Water Resources Planning and Management*, 394–402.

Parry, M.L., Canziani, O.F., Palutikof J.P., van der Linden P.J, & Hanson, C.E. (2007). Summary for Policymakers In: Climate Change 2007: Impacts, adaptation and vulnerability. Contribution of Working Group to the Fourth Assessment Report of the Intergovernmental Panel on Climate Change. Cambridge University Press, Cambridge, UK, 7–22

Rawat, J.S., Biswas, V., & Kumar, M. (2013). Changes in land use/cover using geospatial techniques: a case study of Ramnagar town area, district Nainital, Uttarkhand, India. *Egyptian Journal of Remote Sensing Space Science*, 16, 111–117.

Salimi, S., Ghanbarpour, M.R., Solaimani, K., & Ahmadi, M.Z. (2008). Floodplain Mapping Using Hydraulic Simulation Model in GIS. *Journal of Applied Science*, (4), 660–665.

Sayal, J., Densmore, A.L., & Carboneau, P. (2014). Analyzing the effect of land-use/cover changes at sub-catchment levels on downstream flood peaks: a semi-distributed modeling approach with sparse data. *Catena*, 118, 28–40.

Selby, M.J. (1989). Earth's changing surface. Clarendon Press. Oxford, United Kingdom.

Stonestrom, D.A., Scanlon, B.R., & Zhang, L. (2009). Introduction to special section on impacts of land use change on water resources. *Water Resource Research*, 45(7), 1–3.

Suetsugi, K. (1998). Control of floodwater and improvements of evacuation system for floodplain management. In: Fukuoka S (ed) Floodplain risk management, Proceedings of an international workshop. Hiroshima, 11–13 November 1996, 191–207.

Sulaiman, N.A., Aziz, N.F.A., Tarmizi, N.M., & Samad, A.M. (2014). Integration of Geographic Information System (GIS) and Hydraulic Modelling to simulate Floodplain Inundation Level for Bandar Segamat. IEEE 5th Control and System Graduate Research Colloquium, Aug. 11 – 12.

Tate, E.C., Olivera, F., & Maidment, D. (1999). Floodplain mapping using HEC-RAS and ArcView GIS. The University of Texas at Austin, Austin.

USACE (2002). HEC-GeoRAS software, U.S Department of Defense, Army Corps of Engineers U.S., Institute for Water Resources, Hydrologic Engineering Center, 609 Second Street, Davis, CA.

Van Niekerk, A. (2011). Stellenbosch University Digital Elevation Model Product Description, 2011 edition. Centre for Geographical Analysis, Stellenbosch.

Wagner, P.D., Kumar, S., & Schneider, K. (2013). An assessment of land use change impacts on the water resources of the Mula and Mutha Rivers catchment upstream of Pune, India. *Hydrological Earth Systems and Science*, 17, 2233–2246.

Werner, M.G.F. (2001). Impact of grid size in GIS based flood extent mapping using a 1D flow model. Hydrology, oceans and atmosphere. *Journal of Physics and Chemistry of the Earth*, Part B., 26, 517–522.

Youssef, A.M., Pradhan, B., Gaber, A.F.D., & Buchroithner, M.F. (2009). Geomorphological hazard analysis along the Egyptian Red Sea coast between Safaga and Quseir. *Natural Hazards and Earth System Sciences*, 9, 751–766.

Zubair, A.O. (2006). Change Detection in Land Use and Land Cover Using Remote Sensing Data and GIS: A Case Study of Ilorin and its Environs in Kwara State (M.Sc. Thesis) University of Ibadan, Nigeria.